JOURNAL OF MAGNETIC RESONANCE **135,** 144–155 (1998)
ARTICLE NO. MN981576

^{13}C and ^{15}N—Chemical Shift Anisotropy of Ampicillin and Penicillin-V Studied by 2D-PASS and CP/MAS NMR

Oleg N. Antzutkin,*,[1] Young K. Lee,†,[2] and Malcolm H. Levitt†

*Division of Inorganic Chemistry, Luleå University of Technology, S-971 87 Luleå, Sweden; and †Physical Chemistry Division, Stockholm University, S-10691, Sweden

Received January 13, 1998; revised July 23, 1998

The principal values of the chemical shift tensors of all ^{13}C and ^{15}N sites in two antibiotics, ampicillin and penicillin-V, were determined by 2-dimensional *p*hase *a*djusted *s*pinning *s*ideband (2D-PASS) and conventional CP/MAS experiments. The ^{13}C and ^{15}N chemical shift anisotropies (CSA), and their confidence limits, were evaluated using a Mathematica program. The CSA values suggest a revised assignment of the 2-methyl ^{13}C sites in the case of ampicillin. We speculate on a relationship between the chemical shift principal values of many of the ^{13}C and ^{15}N sites and the β-lactam ring conformation. © 1998 Academic Press

Key Words: **antibiotics; ^{13}C and ^{15}N solid state NMR; CP/MAS; CSA; 2D-PASS.**

INTRODUCTION

Ampicillin and penicillin-V (Scheme 1) belong to a family of β-lactam antibiotics which act by inhibiting the final steps of bacterial cell wall synthesis (*1*). The underlying reason for the varying pharmacological activities of these antibiotics remains unclear. However, it is believed that the conformations of the thiazolidine rings and of the side chain are correlated with the biological activity (*2*).

Dobson and co-workers have reported high-resolution ^{13}C solid-state NMR studies of a series of penicillins (*3–5*), noting a correlation between ^{13}C chemical shifts and molecular structural features available from X-ray diffraction (*6, 7*). However, only the isotropic ^{13}C chemical shifts were measured. To our knowledge, the only reports of ^{15}N chemical shifts of β-lactam antibiotics concern solution-state isotropic shifts (*8*).

The chemical shift anisotropy (CSA) parameters provide a more detailed picture of the electron distribution and can also be correlated with molecular structural features (*9–11*). All six parameters of the chemical shift tensor (three principal values and three angles specifying the principal axis system in a molecular or crystal fixed axes system) can be obtained by single crystal measurements (*12*); however, sufficiently large crystals are not always available. The three principal values of the chemical shift tensor can be measured directly from the sharp singularities of static NMR powder spectra (*12*). This method is straightforward but suffers from low sensitivity. Moreover, for systems with many non-equivalent chemical sites the overlap between different patterns renders the analysis difficult. In addition, static methods are susceptible to perturbations from dipole–dipole couplings.

The CSA parameters can be determined more reliably from the magic-angle-spinning (MAS) sideband pattern (*13*). When the spinning frequency ω_r is comparable to the spread in Larmor frequencies caused by the CSA, the NMR spectrum contains peaks at frequency coordinates $\omega_j^{\mathrm{iso}} + k\omega_r$, where ω_j^{iso} is the isotropic shift frequency of site j, and k is an integer (called the sideband order). The sideband amplitudes may be analyzed to obtain the chemical shift anisotropy (*14, 15*). However, accurate measurement of the asymmetry parameter requires the analysis of many sidebands at low spinning frequencies (*13*). For systems with many sites, the sideband manifolds from different chemical sites overlap, and the analysis becomes difficult.

Various two-dimensional schemes have been designed for separating the isotropic and anisotropic chemical shift information (*16–31*). All these methods retain CSA information while obtaining a clear distinction between the different chemical sites. Recently, we reported the two-dimensional *p*hase *a*djusted *s*pinning *s*ideband (2D-PASS) experiment (*29, 30*) which has a number of advantages over previous two-dimensional schemes. In particular, it may be performed without difficulty on standard magic-angle-spinning NMR equipment, and requires far fewer acquired transients than related methods such as the magic-angle-turning technique (MAT) (*23–26*). A modification of 2D-PASS suitable for quadrupolar nuclei has been reported recently (*31*).

In the present paper, 2D-PASS is used for obtaining the ^{13}C CSA parameters of two antibiotics, ampicillin and penicillin-V. The heavily overlapping sideband manifolds are separated by 2D-PASS, and analyzed to obtain the chemical shift tensor

[1] To whom correspondence should be addressed. E-mail: Oleg.Antzutkin@km.luth.se. Current address until July 1999: Laboratory of Chemical Physics, National Institute of Diabetes and Digestive and Kidney Diseases, National Institutes of Health, Bethesda, MD 20892-0529.

[2] Current address: Quantum Magnetics, 740 Kenamar Court, San Diego, CA 92121.

1090-7807/98 $25.00
Copyright © 1998 by Academic Press
All rights of reproduction in any form reserved.

Phenoxymethylpenicillinic acid (Penicillin – V)

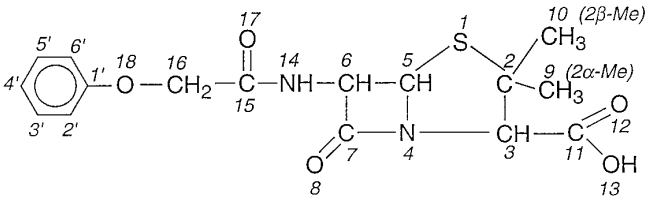

D[–] – α – Aminobenzylpenicillin (Ampicillin)

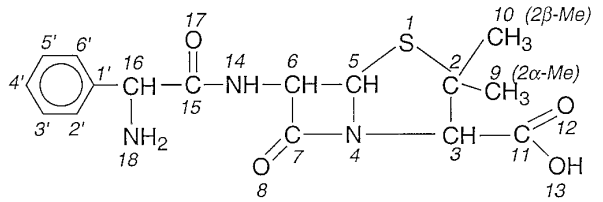

SCHEME 1

principal values of most of the ^{13}C chemical sites. These results suggest that the 2α-methyl and 2β-methyl ^{13}C sites in ampicillin anhydrate powder may have been incorrectly assigned in the literature (*3*). We also performed conventional CP/MAS experiments on ^{15}N sites of these two antibiotics. We speculate on the existence of a correlation between the CSA principal values and the conformation of the five-membered thiazolidine ring.

EXPERIMENTAL SCHEME

The 2D-PASS experimental scheme has been described in Ref. (*29*). It allows the separation of spinning sidebands by order in the ω_1 dimension. The separated spinning sideband patterns may be analyzed by standard numerical procedures to obtain the chemical shift anisotropy parameters.

The 2D-PASS pulse sequence is shown in Fig. 1. Conventional cross polarization from the protons (I-channel) to the carbons (S-channel) (*32*) establishes enhanced ^{13}C transverse magnetization. The PASS sequence of five strong π pulses at specified time delays is then applied under one rotor period. The MAS signal is observed during the time t_2 in the presence of ^{1}H decoupling.

The t_1 incrementation of the 2D scheme is implemented by varying the positions of the π pulses according to numerical solutions of the PASS equations (*29*). Since spinning sidebands are separated by order in ω_1, the number of t_1 increments should exceed the maximum number of sidebands in the MAS spectrum. The π pulse timings for 16 t_1 increments are tabulated in Table 1 of Ref. (*29*). The 2D time domain data matrix is subjected to two complex Fourier transforms to obtain the 2D spectrum. Since the signal is completely cyclic along the t_1 dimension, no special precautions are needed to obtain pure absorption 2D spectra. In particular, hypercomplex data processing, or time-proportional phase incrementation, should *not* be used. When a large number of sidebands is present, a Mathematica program given in Ref. (*29*) calculates the required time-delays enabling an arbitrary fine digitization of the t_1 dimension. Note that the number of t_1 increments does not depend on the desired isotropic shift resolution, in contrast to the related MAT technique (*23–26*).

EXPERIMENTAL

^{13}C CP/MAS and 2D-PASS experiments were performed at a magnetic field of 4.7 T using a Bruker MSL 200 spectrometer. The ^{13}C operating frequency was 50.323 MHz. An external ENI LPI-10H amplifier was employed in the ^{13}C channel of the spectrometer. The RF field corresponded to a ^{13}C nutation frequency of $|\omega^S_{nut}/2\pi| = 116$ kHz. The decoupling power provided a ^{1}H nutation frequency of $|\omega^I_{nut}/2\pi| = 83$ kHz. A

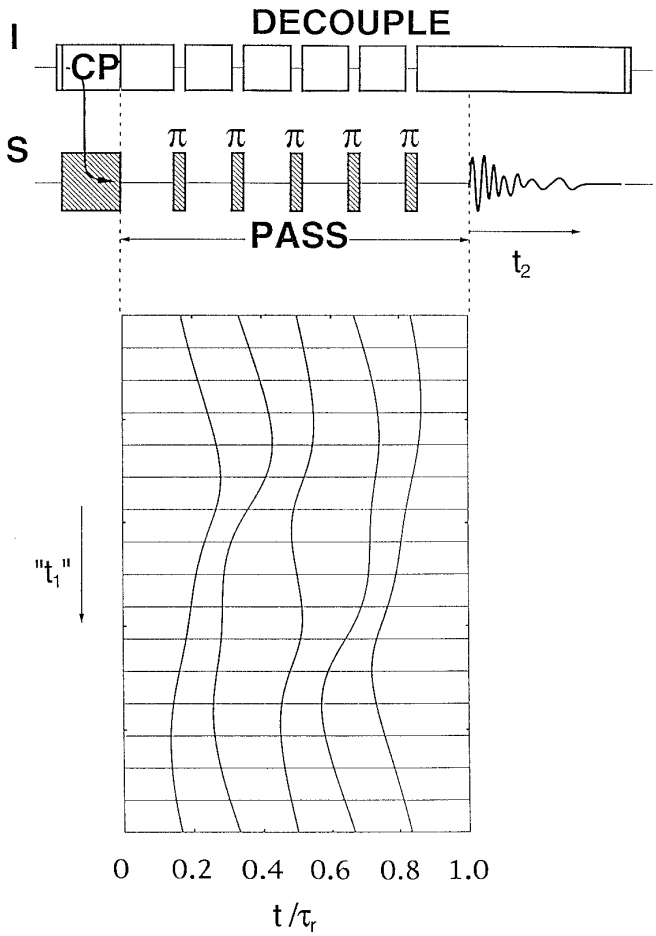

FIG. 1. Pulse sequence for the two-dimensional PASS experiment. The horizontal axis is time in fractions of a rotational period $|2\pi/\omega_r|$. The π pulse timings for the PASS sequences are given in Table 1 of Ref. (*29*). The horizontal cross sections in the insert represent the 16 pulse sequences used in the 2D-PASS experiment.

standard Bruker double bearing 4-mm rotor system (ZrO_2 rotors, Kel-F end caps) was used. The spinning frequency was stabilized to ± 1 Hz using a homebuilt stabilization device controlled by an external PC computer. Both ampicillin (D[−]-α-aminobenzylpenicillin) anhydrate and penicillin-V (phenoxymethyl-penicillinic acid) powder were purchased from Sigma and used without further purification or recrystallization. The cross-polarization interval was 2 ms. The proton RF field was turned off during the ^{13}C π pulses of the PASS sequence to avoid Hartman–Hahn matching. The finite duration of π pulses was accounted for by ensuring that the center of each π pulse was at the timing points tabulated in Table 1 of Ref. (*29*).

The 2D-PASS experiments were run at spinning frequencies of $\omega_r/2\pi = 1030$ Hz and 800 Hz for both penicillin-V and ampicillin. The 1030-Hz experiments employed 972 transients for each t_1 increment, and a relaxation delay of 2 s between transients. The 800-Hz experiments employed 243 transients for each t_1 increment, and a relaxation delay of 1 s between transients.

The effect of pulse imperfections was reduced by using independent phase cycling (*33*) of each π pulse in steps of $2\pi/3$, and adjusting the receiver reference phase, to select the appropriate coherence transfer pathways: $0 \rightarrow (+1) \rightarrow (-1) \rightarrow (+1) \rightarrow (-1) \rightarrow (+1) \rightarrow (-1)$. The total phase cycle was $3^5 = 243$ steps. An integer multiples of 243 transient signals was summed to obtain each t_1 increment of the 2D data matrix. The post-digitization phase shift $\phi_{\text{post dig}}$, the phase ϕ_H of the ^1H $\pi/2$ pulse, the phase ϕ_{CP} of the ^{13}C and ^1H cross-polarization RF fields, the phases $\phi_1, \ldots, \phi_5$ of the π pulses, and the reference phase of the receiver ϕ_{rec}, were varied according to the phase cycle

$$\begin{aligned} \phi_H &= \pi/2 + m\pi \\ \phi_{CP} &= 0 \\ \phi_q &= 2\pi/3 \text{ floor } (3^{1-q}\, m) \\ \phi_{\text{post dig}} &= m\pi \end{aligned} \qquad [1.1]$$

with $q = 1, \ldots, 5$ and ϕ_{rec} adjusted to satisfy the equation

$$\phi_H + \phi_{CP} - 2\phi_1 + 2\phi_2 - 2\phi_3 + 2\phi_4 - 2\phi_5 + \phi_{\text{rec}} + \phi_{\text{post dig}} = \pi/2. \qquad [1.2]$$

Here m is the transient counter, $m = 0, 1, 2, \ldots, 242$, and floor(x) is defined as the largest integer not greater than x. This phase cycle selects ^{13}C signals which are cross-polarized from protons and rejects artifacts from pulse imperfections. A modified 243-step phase cycle which also rejects quadrature receiver imbalance was recently reported (*34*).

The phase shifts reported above (except for $\phi_{\text{post dig}}$) represent the phases of nutation axes in the rotating reference frame. For nuclei of positive magnetogyric ratio, these phases are opposite in sign to the phase shifts generated by the spectrometer electronics (*35*). However, since this particular experiment is unaffected by this sign inconsistency, no special reprogramming of phases is necessary here.

To obtain artifact-free spectra, it was necessary to ensure that the software performs a correct complex Fourier transform in the t_1-dimension. A common software error in commercial systems, associated with incorrect handling of the first data point in the FFT algorithm, leads to weak negative ridges parallel to the ω_1 axis in the 2D spectrum.

Since our 4.7-T magnet has negligible B_0-drift, the experiments were run without a field-frequency lock. More typically, B_0-drift causes spectral ridges parallel to the ω_1 axis in long 2D-PASS experiments. This problem may be avoided by correcting for the magnet drift (either by hardware or by software) or by distributing the acquisition of each t_1 increment over the entire experimental run.

All ^{13}C chemical shifts data were externally referenced to the least shielded resonance of solid adamantane at 38.56 ppm relative to tetramethylsilane (*36*).

Natural abundance ^{15}N CP/MAS spectra were recorded on a Chemagnetics Infinity CMX-360 spectrometer ($B_0 = 8.46$ *T*). The ^{15}N operating frequency was 36.479 MHz. The proton $\pi/2$ pulse duration was 3.2 μs, the CP mixing interval was 3.5 ms, and the nutation frequency of protons during decoupling was 50 kHz. The 8800 or 17,600 transients spaced by relaxation delays of 2 s were accumulated. A standard CMX double bearing 7.5-mm ZrO_2 rotor system was used. The mass of the powder sample was approximately 350 mg. The CP/MAS experiment used a standard 4-step phase cycle. The ^{15}N isotropic chemical shifts are given with respect to NH_4Cl powder (0 ppm, externally referenced) (*37*). The drift of the ^{15}N frequency (B_0-drift) was 0.016 Hz h^{-1}. All solid state ^{13}C and ^{15}N spectra were recorded at room temperature (298 K).

EXPERIMENTAL RESULTS

The ^{13}C CP/MAS spectra of ampicillin and penicillin-V powder spinning at $\omega_r/2\pi = 7000$ Hz are shown in Figs. 2a and 2b, respectively. Almost all ^{13}C resonances are resolved. Most of these resonances are singlets but some of them are broadened and split by ^{13}C-^{14}N dipole–dipole coupling (*38, 39*).

Most of the peak assignments are taken from Clayden *et al.* (*3*) and are based on a comparison of solid-state and solution NMR spectra (*40, 41*). However, the assignment of the 2α-methyl and 2β-methyl peaks in ampicillin (marked by asterisks in Fig. 2a) must be regarded as ambiguous. The two isotropic shifts are only separated by 1.33 ppm. The CSA principal values, reported below, suggest that these two peaks may have been misassigned in Ref. (*3*). In the following discussion, and in Fig. 2a, we employ revised assignment of these two peaks. However, these revised assignments cannot be asserted with complete certainty.

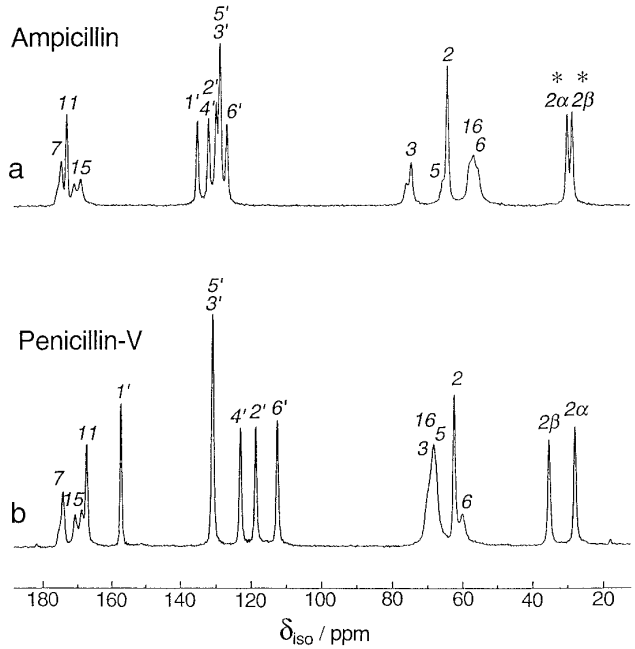

FIG. 2. The ^{13}C CP/MAS spectra of (a) ampicillin and (b) penicillin-V powder at the rotor frequency $|\omega_r/2\pi| = 7000$ Hz (sums of 4800 transients). The assignments of the various carbon resonances are taken from Ref. (*3*), except for the two ampicillin peaks indicated by asterisks, which have reversed assignments.

The remaining assignments were supported by the ^{13}C-^{14}N second order spectral patterns and ^{1}H-^{13}C dipolar dephasing experiments. In the latter, the resonances of protonated carbons, with the exception of rapidly spinning methyl groups, were completely suppressed (*3*). We also performed ^{1}H-^{13}C dipolar dephasing experiments in combination with TOSS sideband suppression experiments (*42*). The decoupler was turned off for a 40-μs interval between the 4th and 5th pulses of the five pulse TOSS sequence (*43*). We observed the suppression of peaks 3, 5, 6, 16, 2′–6′ arising from protonated ^{13}C sites of both penicillin-V and ampicillin powder samples (results not shown). In these experiments, the spinning frequency was $|\omega_r/2\pi| = 1500$ Hz.

Figures 3 and 4 show 2D-PASS spectra of ampicillin and penicillin-V powder spinning at $|\omega_r/2\pi| = 1030$ Hz. The 1D CP/MAS spectra (top) display highly overlapped sideband patterns from the sixteen ^{13}C sites. In the 2D-PASS spectra (middle), the spinning sidebands are separated along the ω_1 dimension according to their order k, and the sidebands for each chemical site lie diagonally in the 2D spectra. Contour plots are also shown (bottom). The relative sideband amplitudes for each chemical site in the 2D spectrum are the same as in the 1D MAS experiment (*29*). Conventional spinning sideband analysis (*15*) may be used to extract the CSA principal values. We also performed 2D-PASS experiments at $|\omega_r/2\pi| =$ 800 Hz (not shown).

Note that the sideband order k increases from left to right in these spectra. This is consistent with the sense of the frequency axis, taking into account the negative sign of the Larmor frequency for nuclei of positive magnetogyric ratio (*35*).

The ^{15}N CP/MAS spectra of ampicillin and penicillin-V powder spinning at $|\omega_r/2\pi| = 1500$ Hz are shown in Figs. 5a and 5b. The peak assignment was based on the observation that the N14 peak is considerably broadened by the heteronuclear ^{1}H–^{15}N dipolar interaction in experiments with a low proton decoupling power. The 2D-PASS experiment was not needed here since spinning sideband manifolds of just two (for penicillin-V) or three (for ampicillin) ^{15}N sites were well separated. CP/MAS experiments at $|\omega_r/2\pi| = 750$ Hz and 617 Hz were also performed (not shown).

The sideband order k increases from right to left in the ^{15}N spectra. This is because the negative sign of the magnetogyric ratio γ leads to a positive nuclear Larmor frequency and hence a spectral frequency coordinate increasing from right to left (*35*).

CSA ANALYSIS

Chemical Shift Definitions

In the discussion below, a *deshielding* convention for chemical shifts is employed throughout. Our usage is specified below, for the sake of clarity. The principal values of the symmetric part of the chemical shift tensor of site j are denoted (δ_{xx}, δ_{yy}, δ_{zz}) and ordered by convention so that

$$|\delta_{zz} - \delta_{iso}| \geq |\delta_{xx} - \delta_{iso}| \geq |\delta_{yy} - \delta_{iso}|, \qquad [1.3]$$

where the isotropic shift is defined

$$\delta_{iso} = (\delta_{xx} + \delta_{yy} + \delta_{zz})/3. \qquad [1.4]$$

The *chemical shift anisotropy* (CSA) δ_{aniso} and *asymmetry parameter* η are defined

$$\delta_{aniso} = \delta_{zz} - \delta_{iso} \qquad [1.5]$$

$$\eta = (\delta_{yy} - \delta_{xx})/(\delta_{zz} - \delta_{iso}). \qquad [1.6]$$

In frequency units, the chemical shift anisotropy may also be written

$$\omega_{aniso} = \omega_0\delta_{aniso}, \qquad [1.7]$$

where ω_0 is the Larmor frequency $\omega_0 = -\gamma B_0$ (including the sign).

Evaluation of CSA Parameters from Sideband Intensities

The spinning sideband intensities $a^{(k)}$ are complicated functions of the shift anisotropy parameters and cannot be ex-

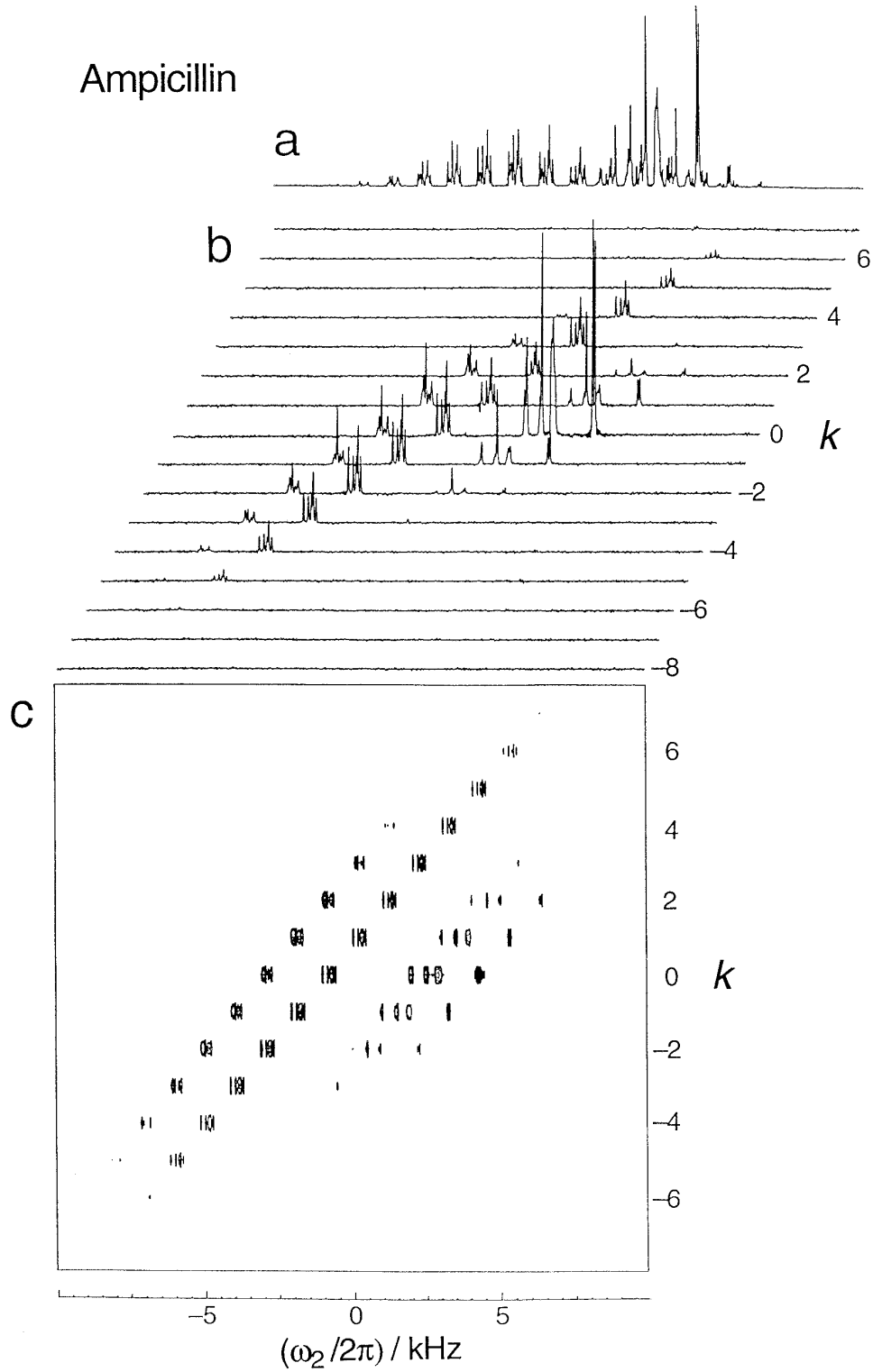

FIG. 3. The ^{13}C spectra of ampicillin powder at the rotor frequency $|\omega_r/2\pi| = 1030$ Hz. (a) The 1D CP/MAS spectrum (15,552 transients). (b) Two-dimensional PASS spectrum showing sidebands separated in the ω_1-dimension. The ω_1-slices are labelled with the sideband order k. A total of 16 t_1 increments were taken, each the sum of 972 transients. (c) The 2D-PASS spectrum presented as a contour plot. For clarity, three rows containing zero signal were inserted between each ω_1-slice.

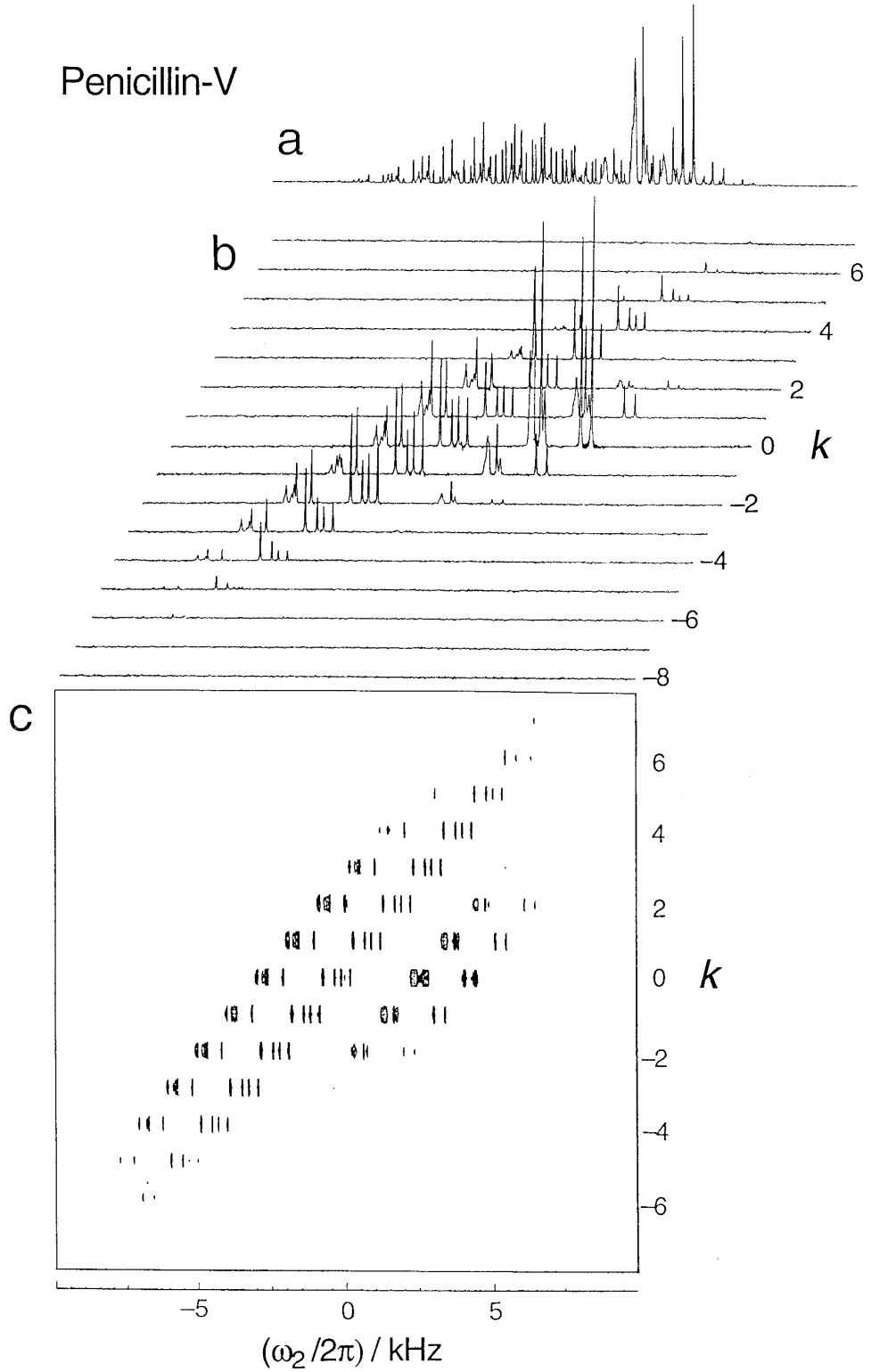

FIG. 4. The ^{13}C spectra of penicillin-V powder. The same conditions as in Fig. 3.

pressed analytically. However, they depend only on the values of the two parameters ω_{aniso}/ω_r and η, making it possible to perform "universal" simulations which may be used for a range of spinning frequencies and magnetic fields. We have developed a computer program for the estimation of CSA parameters from sideband intensities. The program uses a Math-

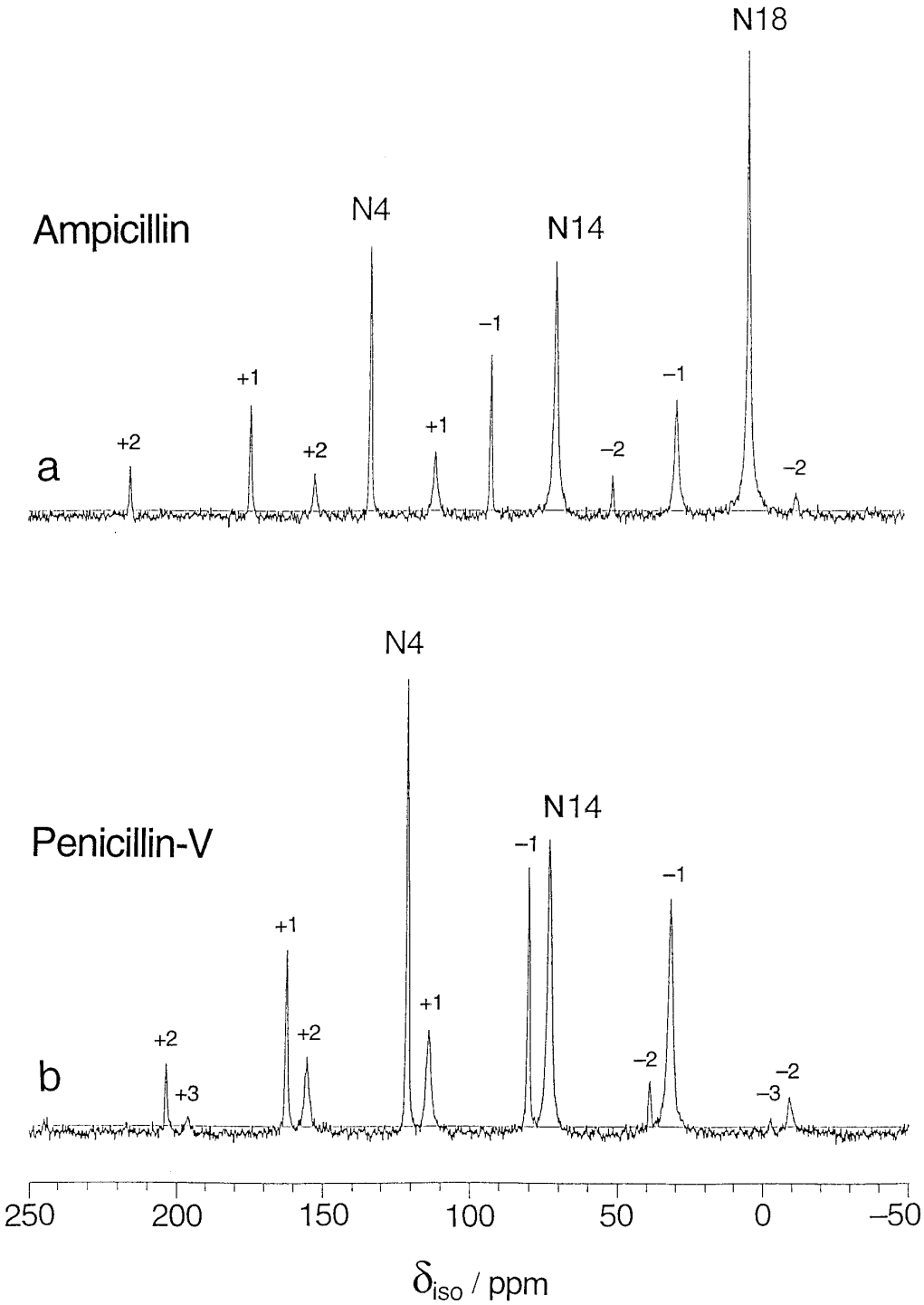

FIG. 5. The ^{15}N CP/MAS spectra of (a) ampicillin (sum of 8800 transients) and (b) penicillin-V (sum of 17,600 transients) powder at the rotor frequency $|2\pi/\omega_r| = 1500$ Hz. The peak assignments and sideband orders are indicated.

ematica front end (*44*), is simple to use, and provides a visual representation of rigorous confidence limits.

A grid of sideband intensity functions of two variables ω_{aniso}/ω_r and η was calculated for sidebands of $-11 \leq k \leq +11$. Instead of frequency domain calculations (*15*), we perform direct time-domain calculations as first suggested by Maricq and Waugh (*14*). FID signals for a single CSA orientation, $s(t, \Omega_{PR})$, were calculated for a set of 64 equally spaced times t in the interval $[0, |2\pi/\omega_r|]$. The Fourier transform of this signal evaluated at the frequencies $k\omega_r$ yields the kth sideband

intensities of a single orientation component, $a^{(k)}(\Omega_{PR})$. Here, the CSA orientation is specified by the three Euler angles $\Omega_{PR} = \{\alpha_{PR}, \beta_{PR}, \gamma_{PR}\}$ characterizing the orientation of the principal axis system of the CSA tensor, P, with respect to a rotor system R fixed on the mechanical rotor, with its z axis along the rotation axis. "Carousel" symmetry (*45*) was used to simplify powder averaging:

$$\langle a^{(k)}_{sim}(\Omega_{PR})\rangle_{\Omega_{PR}} = \left(\frac{1}{4\pi}\right)\int_0^{\pi} d\beta_{PR}\sin\beta_{PR}\int_0^{2\pi} d\alpha_{PR}|a^{(k)}(\alpha_{PR}, \beta_{PR}, 0)|^2. \quad [1.8]$$

The integration was performed by summation over 5000 orientations Ω_{PR}.

We have recently shown that the integration in the Eq. [1.8] need only be performed over one octant of the unit sphere. In addition, we have demonstrated a modified orientational sampling scheme which provides high accuracy using a greatly reduced number of computed orientations (*46*). However, we did not yet incorporate these advances in the results shown here.

For each sideband order $k = -11 \cdots +11$, a matrix of intensities was simulated using 51 ω_{aniso}/ω_r values on the interval [10, −10] and 11 η values on the interval [0, 1]. A Mathematica routine was then used to interpolate these functions. The input file to the Mathematica program consists of the experimental sideband intensities $a^{(k)}_{exp}$, the experimental spinning frequency ω_r, the Larmor frequency ω_0, and the experimental noise variance σ_{noise}. The program plots the chi-square statistic χ^2 as a function of the two chemical shift anisotropy parameters δ_{aniso} and η,

$$\chi^2(\delta_{aniso}, \eta) = \sum_{k=k_{min}}^{k_{max}} \{Aa^{(k)}_{exp} - a^{(k)}_{sim}(\delta_{aniso}, \eta)\}^2/(A\sigma_{noise})^2, \quad [1.9]$$

where A is a vertical-scale parameter. For each pair of CSA parameters (δ_{aniso}, η), the χ^2 statistics are minimized by adjusting the value of A. Usually, the χ^2 surface displays a sharp minimum around some particular CSA values (δ^0_{aniso}, η^0), at which point $\chi^2 = \chi^2_{min}$. Since there are 3 fitting parameters (the two CSA parameters, and the vertical scale parameter A), the value of χ^2_{min} is expected to be around $n_k - 3$, where n_k is the number of sideband amplitudes included in the fit. The joint confidence regions on the two CSA parameters are bounded by the contours $\chi^2 = \chi^2_{min} + 2.3$ (68.3% confidence limit) and $\chi^2 = \chi^2_{min} + 6.17$ (95.4% confidence limit) (*47*). The error limits on the *individual* CSA parameters may be estimated from the projections of the $\chi^2 = \chi^2_{min} + 1$ contour on the two axes (*47*).

The procedure described here does not take into account potential sideband amplitude distortions from orientation-dependent cross-polarization efficiencies or non-uniform molecular orientation distributions. In addition, we did not take into account dipolar interactions with other spins, such as ^{14}N.

This method is more intuitive and more reliable than the graphical plots of sideband amplitude ratios employed in the Herzfeld–Berger procedure (*15*). A similar procedure for determining the CSA parameters was developed by Clayden *et al.* (*48*) and de-Groot *et al.* (*49*). These authors used tables of sideband amplitudes obtained by Bessel function analysis (*15*). Recently Olivieri reported a related error analysis of CSA determinations from spinning sidebands (*50*). A reliability analysis of determined CSA parameters has been given by Hodgkinson *et al.* (*13*).

The Mathematica routine for spinning sideband analysis may be downloaded from the world-wide-web site: http://www.fos.su.se/~mhl.

CHEMICAL SHIFT ANISOTROPIES

We have performed CSA estimations for all resolved ^{13}C and ^{15}N sites of the two antibiotics. Figure 6 shows CSA estimations for six representative ^{13}C sites of penicillin-V. Each plot is a superposition of contour diagrams for two independent $\chi^2(\delta_{aniso}, \eta)$ surfaces, obtained for 2D-PASS experiments at spinning frequencies $|\omega_r/2\pi| = 1030$ Hz (thick lines) and 800 Hz (thin lines). The boundaries of the 68.3% joint confidence region (solid lines) and 95.4% joint confidence region (dashed lines) for the two CSA parameters are shown.

The confidence regions derived from the 800-Hz spectra are generally much larger than for the 1030 Hz spectra. In part, the wide confidence regions at 800 Hz are due to the smaller number of experimental transients accumulated in this case (243 for each t_1 increment, compared to 972 for each t_1 increment at 1030 Hz). For all sites, the 68.3% confidence regions for the two different spinning frequencies overlap.

The 68.3% confidence limits on the *individual* parameters δ_{aniso} and η may be derived from the projections of the $\chi^2 = \chi^2_{min} + 1$ contour on the two axes (*47*). The CSA estimations and confidence limits derived from 1030-Hz 2D-PASS spectra are given in Table 1 (for ampicillin) and Table 2 (for penicillin-V). In principle, the estimations at different spinning frequencies could be combined using Z-surfaces (*11*).

The estimated CSA parameters for the ^{13}C sites which are directly bonded to ^{14}N are significantly perturbed by the $^{13}C \cdots {}^{14}N$ dipolar coupling. The tabulated values do not take this contribution into account.

There is a small discrepancy of 0.28 ppm between the isotropic chemical shifts given in Tables 1 and 2 and those given by Clayden *et al.* (*3*). This discrepancy is due to a deviation in the adamantane chemical shift reference reported by Earl *et al.* (*36*) and that used by Clayden *et al.* (*3*). We have verified that the adamantane chemical shifts are 38.56 ± 0.03 ppm and 29.51 ± 0.03 ppm relative to TMS in agreement with Earl *et al.* (*36*).

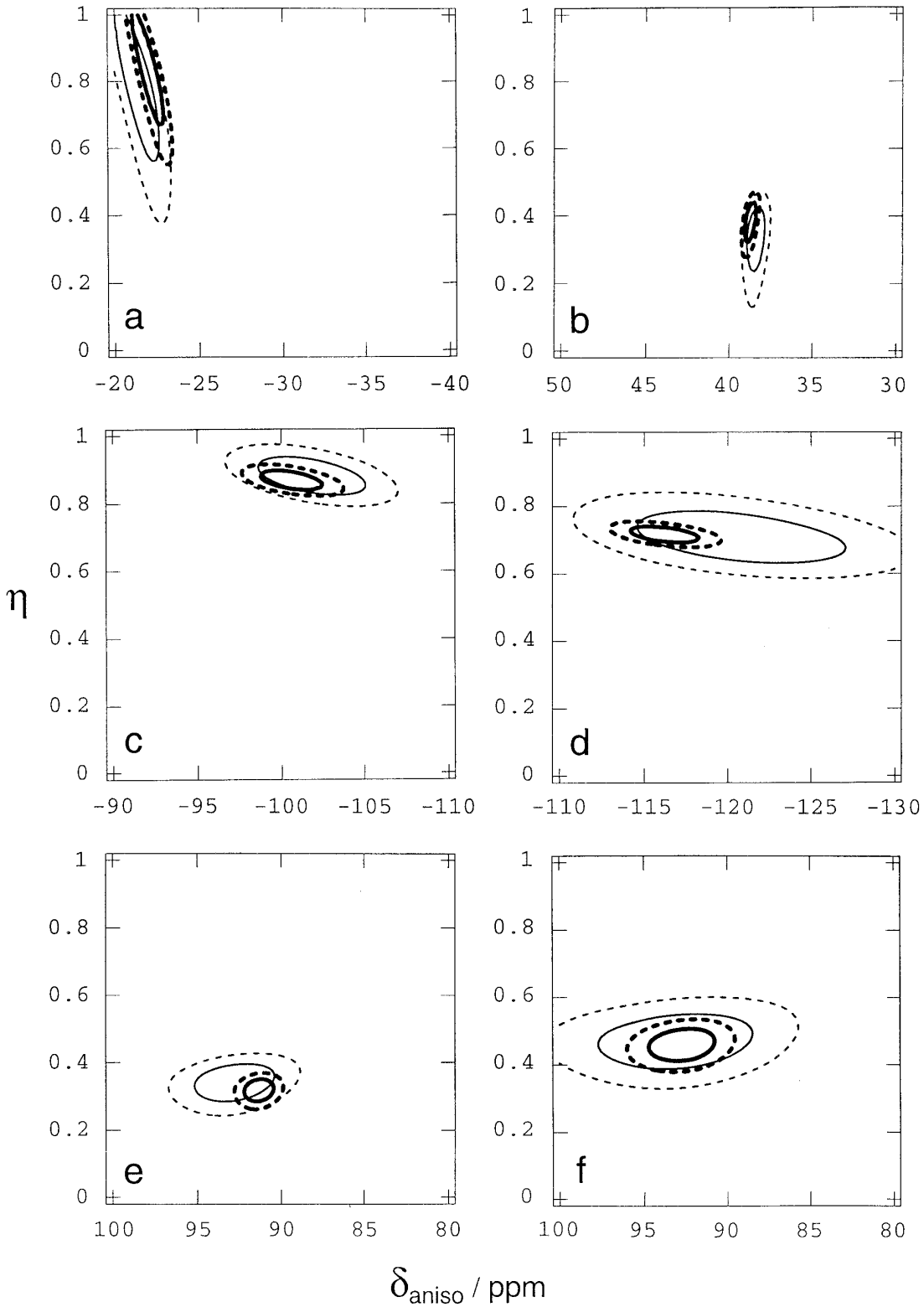

FIG. 6. χ^2 statistic as a function of the CSA parameters δ_{aniso} and η (Penicillin-V, 2D-PASS, spinning frequencies 1030 Hz (thick lines), and 800 Hz (thin lines)). Graphs for six representative ^{13}C sites are presented: (a) 2α-Me, (b) C2, (c) phenyl C1′, (d) phenyl C4′, (e) carboxyl C11, and (f) carbonyl C7. The 68.3% joint confidence limit (solid) and 95.4% joint confidence limit (dashed) for the two CSA parameters are shown.

TABLE 1
^{13}C and ^{15}N Shielding Parameters in Ampicillin (in ppm)

Carbon site[a]	δ_{iso} (from TMS)	δ_{aniso}	η
2β-Me*	28.9 ± 0.1	−28.6 ± 0.5	0.56 ± 0.08
2α-Me*	30.2 ± 0.1	−22.9 ± 0.5	0.94 ± 0.06
C6, C16	57 ± 1[b]	overlapped	
C2	64.8 ± 0.1	42.0 ± 0.3	0.76 ± 0.02
C5	65.3 ± 0.5[b]	36.5 ± 2.9	0.66 ± 0.29
C3	73.4 ± 0.5[b]	−31.6 ± 0.7	0.60 ± 0.11
C6′	127.1 ± 0.1	−116.9 ± 1.3	0.64 ± 0.02
C3′, C5′	129.2 ± 0.1	−115.3 ± 0.4	0.72 ± 0.01
C2′	130.0 ± 0.1	−104.6 ± 1.0	0.79 ± 0.02
C4′	132.3 ± 0.1	−121.9 ± 1.5	0.68 ± 0.02
C1′	135.5 ± 0.1	−115.5 ± 1.0	0.61 ± 0.02
C15	170.1 ± 0.5[b]	89.1 ± 2.0	0.73 ± 0.04
C11	173.3 ± 0.1	67.1 ± 0.7	0.93 ± 0.02
C7	175.2 ± 0.5[b]	93.2 ± 1.5	0.53 ± 0.04
Nitrogen site	**δ_{iso} (from NH_4Cl)**	**δ_{aniso}**	**η**
N4	133.1 ± 0.1	91.5 ± 4.0	0.69 ± 0.04
N14	70.0 ± 0.1	87.5 ± 3.5	0.25 ± 0.13
N18	4.2 ± 0.1	10 ± 5	uncertain

[a] Assignments taken from Ref. (*3*), except for the 2α-Me and 2β-Me sites (marked by *).
[b] The ^{13}C–^{14}N doublets. The estimated CSA values are influenced by ^{13}C–^{14}N dipolar couplings.

The ^{15}N chemical shift anisotropies were estimated from one-dimensional MAS spectra at spinning frequencies of $\omega_r/2\pi$ = 617, 750, and 1500 Hz. In this case, the overlap between the 68.3% joint confidence regions at the different spinning frequencies was used to estimate the error limits.

In Fig. 7, we compare the experimental and simulated sideband amplitudes for the carboxyl C11 site of penicillin-V at spinning frequencies of $\omega_r/2\pi$ = 800 and 1030 Hz. The error bars on the experimental points indicate the standard deviation of the noise. For the simulated spectra the parameters δ_{aniso} and η were taken from Table 2. Similar agreement was obtained for most of the ^{13}C sites. Larger deviations, however, were obtained for ^{13}C sites directly bonded to nitrogen. The heteronuclear $^{13}C \cdots {}^{14}N$ dipolar coupling perturbs the spinning sideband amplitudes, and in addition leads to broadenings and splittings, since ^{14}N has a strong quadrupolar interaction (*38, 39*). The peak broadening causes overlap with other peaks, and reduced signal-to-noise ratio for these sites. These factors are reflected in the wider confidence limits for the N-bonded ^{13}C sites (see, for example, Fig. 6f).

DISCUSSION

Single-crystal X-ray analyses have shown that the five-membered thiazolidine ring S1–C2–C3–N4–C5– exists in one of two non-planar conformations, called C-3 or S-1. The notation indicates which atom is significantly displaced from the plane defined by the other four atoms (*51*). Penicillin-V is in the C-3 conformation in the solid state, while ampicillin-V is in the S-1 conformation (*6, 7*).

Clayden *et al.* postulated a correlation between the ^{13}C isotropic chemical shift of the 2β-methyl site and the thiazolidine ring conformation (*3*). The ^{13}C isotropic chemical shift of the 2β-Me site is δ_{iso} = 36 ppm for C-3 penicillins and δ_{iso} = 29.5 ppm for S-1 penicillins (*3*). Similarly, penicillin-V (C-3 conformation) has δ_{iso}(2β-Me) = 35.3 ± 0.1 ppm while ampicillin (S-1 conformation) has δ_{iso}(2β-Me) = 28.9 ± 0.1 ppm (see Tables 1 and 2). These chemical shift changes were attributed to the influence of the β-lactam carbonyl group (C7): the 2β-Me-C7 separations in the C-3 and S-1 puckers are approximately 0.35 and 0.45 nm, respectively (*3*).

In the spectrum of ampicillin Clayden *et al.* assigned the resonance at δ_{iso} = 28.9 ppm to the 2α-Me site and the resonance at δ_{iso} = 30.2 ppm to the 2β-Me site (*3*). These assignments were based on a comparison of solid-state and solution NMR spectra (*40, 41*). However, some of these assignments may be challenged, since the shift differences are small, and comparable to shifts which are typically observed when passing from the solution to the solid state. The CSA parameters in Tables 1 and 2 suggest a revised assignment in the case of ampicillin: δ_{iso}(2α-Me) = 30.2 ppm and δ_{iso}(2β-Me) = 28.9 ppm. The new assignment allows the chemical shift anisotropy and the asymmetry parameter of both Me sites to be roughly preserved when the thiazolidine ring conformation is changed. Nevertheless, the reassignment is not beyond doubt, since the CSA parameters are known to be conformation-sensitive, as discussed below.

TABLE 2
^{13}C and ^{15}N Shielding Parameters in Penicillin-V (in ppm)

Carbon site[a]	δ_{iso} (from TMS)	δ_{aniso}	η
2α-Me	27.9 ± 0.1	−22.0 ± 0.6	0.84 ± 0.11
2β-Me	35.3 ± 0.1	−29.6 ± 0.4	0.63 ± 0.06
C6	61.1 ± 0.5[b]	40.1 ± 0.8	0.62 ± 0.09
C2	62.5 ± 0.1	38.7 ± 0.2	0.40 ± 0.02
C3, C5, C16	69 ± 1[b]	overlapped	
C6′	112.6 ± 0.1	−101.0 ± 0.7	0.59 ± 0.01
C2′	118.6 ± 0.1	−95.4 ± 0.6	0.69 ± 0.01
C4′	123.0 ± 0.1	−116.3 ± 1.2	0.72 ± 0.02
C3′, C5′	130.8 ± 0.1	−118.5 ± 0.7	0.67 ± 0.01
C1′	157.3 ± 0.1	−90.6 ± 1.2	0.87 ± 0.02
C11	167.3 ± 0.2	91.3 ± 0.6	0.32 ± 0.02
C15	169.8 ± 0.5[b]	83.4 ± 1.8	0.88 ± 0.03
C7	174.4 ± 0.5[b]	92.7 ± 1.3	0.46 ± 0.03
Nitrogen site	**δ_{iso} (from NH_4Cl)**	**δ_{aniso}**	**η**
N4	121.4 ± 0.1	92.4 ± 4.0	0.65 ± 0.07
N14	73.2 ± 0.1	105.5 ± 4.0	0.15 ± 0.15

[a] Assignments taken from Ref. (*3*).
[b] The ^{13}C–^{14}N doublets. The estimated CSA values are influenced by ^{13}C–^{14}N dipolar couplings.

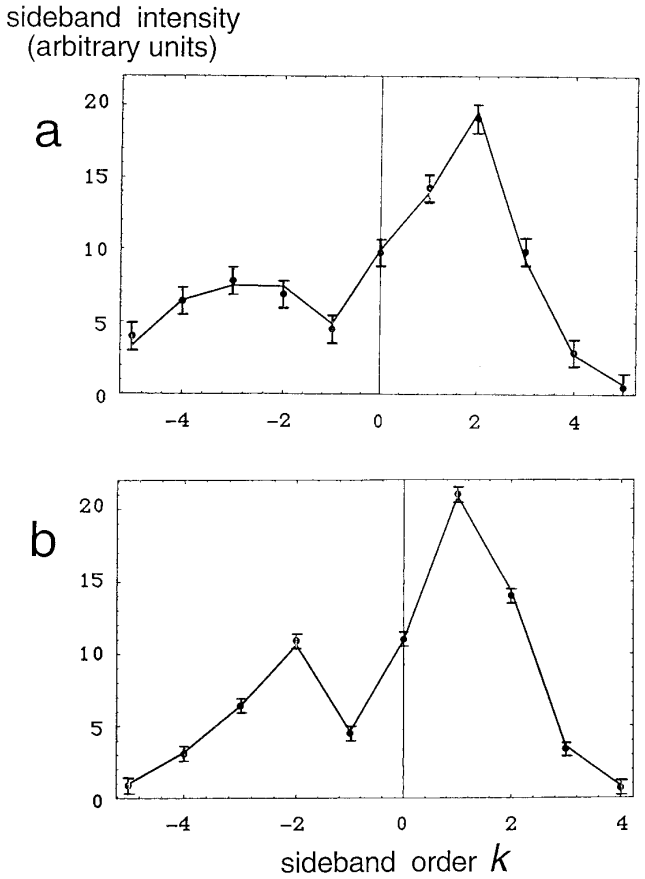

FIG. 7. Experimental (dots) and simulated (connected lines) sideband amplitudes of the carboxyl C11 site of penicillin-V. The spinning frequency is (a) 800 Hz, (b) 1030 Hz. Simulations are performed with parameters δ_{aniso} and η from Table 2. The error bars indicate the measured noise variance.

Many of the shielding anisotropies are quite different for ampicillin and penicillin-V, even in formally identical parts of the molecule. This may be due to the conformation of the thiazolidine ring, although the influence of intermolecular interactions cannot be excluded. For example, the asymmetry parameter η of the C2 site differs significantly in the two molecules ($\eta = 0.76 \pm 0.02$ in ampicillin and $\eta = 0.40 \pm 0.02$ in penicillin-V). The CSA parameters of the carboxyl site C11 are also very different for the two antibiotics ($\delta_{aniso} = 67.1 \pm 0.7$, $\eta = 0.93 \pm 0.02$ in ampicillin and $\delta_{aniso} = 91.3 \pm 0.6$, $\eta = 0.32 \pm 0.02$ in penicillin-V).

The shielding parameters of the carbonyl site, C7, coincide within error limits for the two compounds suggesting a similar electronic environment in this part of the molecule. This is also true for the carbonyl C15 site. There is a large variation in isotropic chemical shifts for the N4 nitrogen site of the β-lactam ring ($\delta_{iso} = 133.1 \pm 0.1$ in ampicillin and $\delta_{iso} = 121.4 \pm 0.1$ in penicillin-V), while the CSAs are quite similar. This might be due to a conformation-dependent change in electron density at the ^{15}N nucleus, while preserving the local pyramidal geometry of the electronic orbitals. The other ring sites, C3, C5, and C6, are inaccessible for the comparative analysis because of peak overlap in our relatively low magnetic field.

Apart from the C1′ site of penicillin-V which is directly attached to oxygen O18, all aromatic carbons have similar CSAs with large δ_{aniso} around -110 ppm and η between 0.6 and 0.8. There is no indication of significant internal motion of the benzene ring in ampicillin and penicillin-V molecules at room temperature: Peaks from sites 2′ and 6′, and from 3′ and 5′, are individually resolved, allowing rapid ring flips to be ruled out. There is no indication of broadening which would arise from motion on a millisecond time scale.

Since we have only studied two systems so far, the above correlations between CSA values and thiazolidine ring conformation have to be regarded as speculative. Such correlations might be established by theoretical calculations of CSA tensors. There has been recent progress in establishing similar correlations in peptides and proteins (*10*). In the future we also plan to study a range of penicillin systems in order to test our conclusions.

CONCLUSIONS

We have measured ^{13}C chemical shift anisotropy for 13 of the 16 carbon and for two ^{15}N sites of two antibiotics, ampicillin and penicillin-V. The 2D-PASS method was used to separate the heavily overlapping ^{13}C spinning sideband manifolds. The separated sideband patterns were analyzed by numerical simulations using a Mathematica program and the CSA parameters were obtained together with error limits.

The CSA values suggest a revised assignment of the 2-methyl ^{13}C peaks in the case of ampicillin.

The CSAs of many sites in ampicillin and penicillin-V were found to display significant differences, which may be associated with the thiazolidine ring conformation. The ^{13}C shielding anisotropy parameters show a wider variation than the isotropic shifts.

ACKNOWLEDGMENTS

This work has been supported by the Swedish Natural Science Research Council, and the Göran Gustafsson Foundation for Research in the Natural Sciences and Medicine. The CMX-360 spectrometer (Luleå University of Technology) was purchased with a grant from Swedish Council for Planning and Coordination of Research (FRN). We thank T. Karlsson and O. G. Johannessen for construction of a spinning frequency stabilizer and one of the reviewers for stimulating criticism.

REFERENCES

1. "β-Lactam Antibiotics, Chemistry and Biology" (R. B. Morin and M. Gorman, Eds.), Academic Press, New York (1981).
2. N. C. Cohen, *J. Med. Chem.* **26,** 259 (1983).
3. N. J. Clayden, C. M. Dobson, L-Y. Lian, and J. M. Twyman, *J. Chem. Soc. Perkin Trans. 2,* 1933 (1986).
4. J. M. Twyman and C. M. Dobson, *J. Chem. Soc. Chem. Commun.,* 786 (1988).

5. J. M. Twyman, J. Fattah, and C. M. Dobson, *J. Chem. Soc. Chem. Commun.,* 647 (1991).
6. S. Abrahamson, D. C. Hodgkin, and E. N. Maslen, *Biochem. J.* **86,** 514 (1963).
7. M. O. Boles and R. J. Girven, *Acta Crystallogr. Sect. B* **32,** 2279 (1976).
8. J. W. Paschal, D. E. Dorman, P. R. Srinivasan, and R. L. Lichter, *J. Org. Chem.* **43**(10), 2013 (1978).
9. W. S. Veeman, *Progr. NMR Spectrosc.* **16,** 193 (1984).
10. A. C. deDios and E. Oldfield, *Solid State Nucl. Magn. Reson.* **6,** 101 (1996).
11. J. Heller, D. D. Laws, M. Tomaselli, D. S. King, D. E. Wemmer, A. Pines, R. H. Havlin, and E. Oldfield, *J. Am. Chem. Soc.* **119,** 7827 (1997).
12. D. M. Grant, Chemical shift tensors, *in* "Encyclopedia of Nucl. Magn. Reson." (D. M. Grant, Ed.), p. 1298, Wiley, New York (1996).
13. P. Hodgkinson and L. Emsley, *J. Chem. Phys.* **107,** 4808 (1997).
14. M. M. Maricq and J. S. Waugh, *J. Chem. Phys.* **70,** 3300 (1979).
15. J. Herzfeld and R. G. Berger, *J. Chem. Phys.* **73,** 6021 (1980).
16. Y. Yarim-Agaev, P. M. Tutunjian, and J. S. Waugh, *J. Magn. Reson.* **47,** 51 (1982).
17. A. Bax, N. M. Szeverenyi, and G. E. Maciel, *J. Magn. Reson.* **51,** 400 (1983).
18. R. Tycko, G. Dabbagh, and P. Mirau, *J. Magn. Reson.* **85,** 265 (1989).
19. A. Bax, N. M. Szeverenyi, and G. E. Maciel, *J. Magn. Reson.* **55,** 494 (1983).
20. T. Terao, T. Fujii, T. Onodera, and A. Saika, *Chem. Phys. Lett.* **107,** 145 (1984).
21. L. Frydman, G. C. Chingas, Y. K. Lee, P. J. Grandinetti, M. A. Eastman, G. A. Barrall, and A. Pines, *J. Chem. Phys.* **97,** 4800 (1992).
22. A. C. Kolbert and R. G. Griffin, *Chem. Phys. Lett.* **166,** 87 (1990).
23. Z. Gan, *J. Am. Chem. Soc.* **114,** 8307 (1992).
24. J. Z. Hu, D. W. Alderman, C. Ye, R. J. Pugmire, and D. M. Grant, *J. Magn. Reson. A* **105,** 82 (1993).
25. J. Z. Hu, A. M. Orendt, D. W. Alderman, R. J. Pugmire, C. Ye, and D. M. Grant, *Solid State Nucl. Magn. Reson.* **3,** 181 (1994).
26. J. Z. Hu, W. Wang, F. Liu, M. S. Solum, D. W. Alderman, R. J. Pugmire, and D. M. Grant, *J. Magn. Reson. A* **113,** 210 (1995).
27. S. F. de Lacroix, J. J. Titman, A. Hagemeyer, and H. W. Spiess, *J. Magn. Reson.* **97,** 435 (1992).
28. J. J. Titman, S. F. de Lacroix, and H. W. Spiess, *J. Chem. Phys.* **98,** 3816 (1993).
29. O. N. Antzutkin, S. C. Shekar, and M. H. Levitt, *J. Magn. Reson. A* **115,** 7 (1995).
30. W. A. Dollase, M. Feike, H. Förster, T. Schaller, I. Schnell, A. Sebald, and S. Steuernagel, *J. Am. Chem. Soc.* **119**(16), 3807 (1997).
31. D. Massiot, V. Montaillout, F. Fayon, P. Florian, C. Bessada, *Chem. Phys. Lett.* **272,** 295 (1997).
32. A. Pines, M. G. Gibby, and J. S. Waugh, *J. Chem. Phys.* **56,** 1776 (1972).
33. G. Bodenhausen, H. Kogler, and R. R. Ernst, *J. Magn. Reson.* **58,** 370 (1984).
34. Z. Song, O. N. Antzutkin, A. Rupprecht, and M. H. Levitt, *Chem. Phys. Lett.* **253,** 349 (1996).
35. M. H. Levitt, *J. Magn. Reson.* **126,** 164 (1997).
36. W. L. Earl and D. L. VanderHart, *J. Magn. Reson.* **48,** 35 (1982).
37. C. I. Rateliffe, J. A. Ripmeester, and J. S. Tse, *Chem. Phys. Lett.* **99,** 177 (1983).
38. J. G. Hexem, M. H. Frey, and S. J. Opella, *J. Chem. Phys.* **77,** 3847 (1982).
39. A. C. Olivieri, *Solid State Nucl. Magn. Reson.* **1,** 345 (1992).
40. R. Mondelli and P. Ventura, *J. Chem. Soc. Perkin Trans. 2,* 1749 (1977).
41. C. Chang and S. L. Hen, *J. Pharm. Sci.* **68,** 64 (1979).
42. D. P. Raleigh, E. T. Olejniczak, S. Vega, and R. G. Griffin, *J. Magn. Reson.* **72,** 238 (1987).
43. Z. Song, O. N. Antzutkin, X. Feng, and M. H. Levitt, *Solid State Nucl. Magn. Reson.* **2,** 143 (1993).
44. S. Wolfram, "The Mathematica Book," 3rd ed., Wolfram Media/ Cambridge Univ. Press, Cambridge, UK (1996).
45. M. H. Levitt, *J. Magn. Reson.* **82,** 427 (1989).
46. M. Edén and M. H. Levitt, *J. Magn. Reson.* **132,** 220 (1998).
47. W. H. Press, S. A. Teukolsky, W. T. Vetterling, and B. P. Flannery, "Numerical Recipes in C," p. 697, Cambridge Univ. Press, Cambridge, UK (1994).
48. N. J. Clayden, C. M. Dobson, L. Y. Lian, and D. J. Smith, *J. Magn. Reson.* **69,** 476 (1986).
49. H. J. M. de-Groot, S. O. Smith, A. C. Kolbert, J. M. L. Courtin, C. Winkel, J. Lugtenburg, J. Herzfeld, and R. G. Griffin, *J. Magn. Reson.* **91,** 30 (1991).
50. A. C. Olivieri, *J. Magn. Reson. A* **123,** 207 (1996).
51. R. M. Sweet, *in* "Cephalosporins and Penicillins" (E. H. Flynn, Ed.), p. 281, Academic Press, New York (1972).